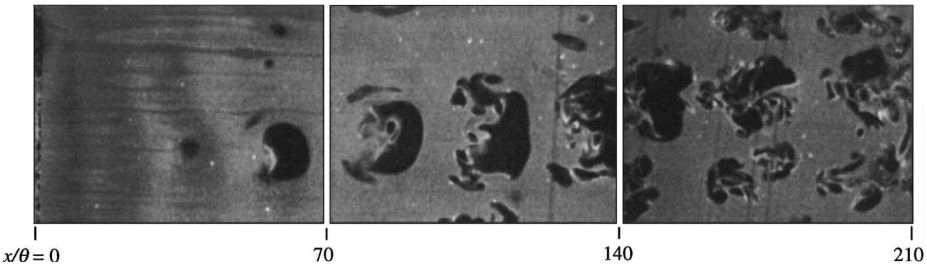

Fig. 4 Uncorrelated plan-view PLS images. (Laser sheet is tilted at a 3-deg angle.)

At the top of the middle image, there is a region that is highly three dimensional. This is believed to be due to contamination from turbulence that originated from the outer regions of the upstream splitter plate boundary layers. We believe that the outboard regions of the splitter plate boundary layers were forced to undergo transition by the unsteady plate/side wall corner vortices.

Plan-view PLS images are shown in Fig. 4 where the laser sheet was rotated about the z axis by about 3 deg, thus allowing the visualization of the outer part of the wake. The upstream half of the leftmost image reveals primarily two-dimensional light and dark bands. In this region the laser sheet does not pass through the laminar wake but just outside of it. The initial spanwise bands at left distort with downstream distance, after which dark round islands of wake fluid appear. The dark islands apparently result from the bending and uplifting of the spanwise vortices. The second image downstream shows that the spanwise vortices become highly three dimensional and sometimes form a horseshoe-shaped structure. The horseshoe-shaped structures are similar to those seen in incompressible flat plate wakes[2] and in numerical simulations of compressible planar wakes.[1]

IV. Conclusions

A preliminary experimental study has been conducted of the laminar-to-turbulent transition of a Mach 3 flat plate wake. Side-view PLS images reveal a vortex street that is remarkably similar to that found under incompressible conditions. Plan-view images show that the initially two-dimensional vortex street rapidly develops both small- and large-scale, three-dimensional instabilities. The effect of the large-scale instability is to cause the spanwise vortices to distort into horseshoe-shaped structures. Furthermore, unlike incompressible wakes, the side-view images reveal that the vortices generate weak eddy shocklets for supersonic relative Mach numbers.

Acknowledgment

We would like to thank James Kendall (Jet Propulsion Laboratory) for providing us with a detailed description of some of his unpublished work on flat plate supersonic wakes.

References

[1]Chen, J. H., Cantwell, B. J., and Mansour, N. N., "The Effect of Mach Number on the Stability of a Plane Supersonic Wake," *Physics of Fluids A*, Vol. 2, No. 6, 1990, pp. 984–1004.

[2]Meiburg, E., and Lasheras, J., "Experimental and Numerical Investigation of the Three-Dimensional Transition in Plane Wakes," *Journal of Fluid Mechanics*, Vol. 190, 1988, pp. 1–37.

[3]Clemens, N. T., Smith, M. F., and Fernandez, J. V., "Observations of Supersonic Flat Plate Wake Transition," AIAA Paper 96-0785, Jan. 1996.

[4]Smith, K. M., and Dutton, J. C., "Large-Scale Structures in Supersonic Reattaching Shear Flows," AIAA Paper 95-2251, June 1995.

[5]Alvi, F. S., Krothapalli, A., and Washington, D., "Fluctuating Pressure Measurements in a Highly Compressible Countercurrent Turbulent Shear Layer," AIAA Paper 95-2175, Jan. 1995.

[6]Vreman, B., Kuerten, H., and Geurts, B., "Shocks in DNS of the Three-Dimensional Mixing Layer," Proceedings of the Tenth Symposium on Turbulent Shear Flows, Pennsylvania State Univ., 1995.

[7]Dimotakis, P. E., "Turbulent Free Shear Layer Mixing and Combustion," *High-Speed Flight Propulsion Systems*, edited by S. N. B. Murthy and E. T. Curran, Vol. 137, Progress in Astronautics and Aeronautics, AIAA, Washington, DC, 1991, pp. 265–340.

W. Oberkampf
Associate Editor

Interaction of Large Three-Dimensional Eddies and Small Streamwise Vortices

Roy Y. Myose*
Wichita State University, Wichita, Kansas 67260-0044
and
Ron F. Blackwelder†
University of Southern California, Los Angeles, California 90089-1191

Introduction

PAST studies have shown that at least two types of organized structures exist in turbulent boundary layers.[1,2] In the outer region are large-scale motions on the size of the boundary-layer thickness δ. Near the wall are small-scale, low- (and high-) speed streamwise streaks, and viscous ($^+$) scaling with the kinematic viscosity ν and friction velocity u_τ is used for these small-scale structures. In a sequence of events called the bursting process, the low-speed streaks lift up off the wall, oscillate, and then break down.[3] This bursting process is responsible for most of the turbulent energy production near the wall.[4] The evolution and breakdown of streamwise vortices are thought to be closely associated with the structure and breakdown of the bursting process.[5,6] In the outer region, the large-scale motion consists of $-\omega_z$ spanwise vortical motion, which entrains nonturbulent fluid from outside the boundary layer.[7,8] At the upstream interface between turbulent and nonturbulent regions, there is an outward movement of fluid away from the wall ahead of the interface and an insweep of high-speed fluid toward the wall behind the interface.[8,9]

In flow visualization studies,[10–12] the bursting process was often followed by an insweep of high-speed fluid. This suggests an interactive relationship between near-wall and outer-region structures. However, both structures appear randomly in space and time, which makes it difficult to study their exact interactive relationship. To address this issue, Myose and Blackwelder[13] devised an experiment to emulate these structures with the proper size and strength but in a deterministic and periodic manner. Reference 13 used Görtler streamwise vortices to emulate the near-wall structure and large two-dimensional spanwise vortices shed from a pitch oscillating airfoil to emulate the outer-region structure. The near-wall vortices initially became unstable due to the normal and spanwise inflectional velocity profiles associated with the wall vortices. Breakdown of the wall vortices was subsequently triggered by the arrival of high-speed fluid associated with the outer region. Increasing the large spanwise vor-

Presented as Paper 97-0442 at the AIAA 35th Aerospace Sciences Meeting, Reno, NV, Jan. 6–9, 1997; received June 20, 1997; revision received February 18, 1998; accepted for publication March 9, 1998.

*Associate Professor, Department of Aerospace Engineering. Associate Fellow AIAA.

†Professor, Department of Aerospace Engineering. Associate Fellow AIAA.

tex strength hastened the breakdown of the wall vortices. These results suggest that the outer region plays a role in the bursting process.

Two-dimensional spanwise vortices were originally used in Ref. 13 to emulate the outer-region structure. The resulting response by the near-wall vortices was relatively uniform in the spanwise direction. According to Cantwell[1] and others, the outer region of the turbulent boundary layer consists of three-dimensional eddies of finite spanwise width. A natural question that arises is whether the near-wall vortices would respond differently to three-dimensional outer eddies. The goal of the present experiment is to address this question.

Experimental Technique

Figure 1 shows the experimental situation and emulation method used. The University of Southern California Görtler wind tunnel[6] was used. Counter-rotating streamwise vortex pairs form and develop in the laminar boundary layer (which is about 1 cm thick at $x = 80$ cm) along the concave wall due to the Görtler instability mechanism. It has been shown that Görtler vortical flow behavior is an excellent emulation of turbulent boundary-layer, near-wall behavior.[6] Only one pair of Görtler streamwise vortices is shown, although in reality there are many pairs with a wavelength λ of about 1–2 cm.

A 36-cm-chord-length NACA 0009 symmetric airfoil was pitch oscillated to produce large (spanwise-oriented) vortical eddies, which were convected downstream. These eddies were produced in the freestream and allowed to interact with the Görtler streamwise vortices on the concave wall. The large vortical eddies encompassed the test section channel width of 15 cm, thus emulating a turbulent boundary layer (TBL) thickness of $\delta_{\text{emulated}} = 15$ cm. The eddy's streamwise length was $3.5\delta_e$ (compared to δ–3δ for TBL[1]), and the streamwise spacing between eddies was $7\delta_e$ (compared to 2δ–9δ for TBL[1]). To produce three-dimensional eddies, the oscillating airfoil incorporated a sawtooth trailing-edge shape with a 7.5-cm extension at the sawtooth tip, i.e., 43.5-cm chord, no extension at the sawtooth valley, and spanwise distance between sawtooth tips of 15 cm, i.e., equal to δ_e. Otherwise, the experimental conditions of Ref. 13 were used. The freestream velocity was $U_\infty = 500$ cm/s, and the airfoil was oscillated sinusoidally with a ±2-deg amplitude and 5-Hz ± 0.1% frequency.

Flow visualization was accomplished by introducing a sheet of smoke at $x = 21.5$ cm and $y = 0.14$ cm using the smoke-wire technique.[6] The resulting smoke patterns were then videotaped. Streamwise velocity measurements were also taken using hot-wire anemometry. The phase angle ϕ of the large outer eddy was determined using a sensor mounted on the airfoil driving mechanism. At the start of each oscillation cycle, the sensor produced a visible indication via a light-emitting diode (LED) and an electronic pulse for data acquisition input. The start of airfoil pitchdown was defined as $\phi = 0$. Using the sensor signal, the phase angle at any given downstream distance was calculated using the large outer eddy's measured convection velocity (equal to U_∞). The measured instantaneous velocity u was decomposed into three parts: the time-averaged portion $\bar{u}$, the periodic portion $\tilde{u}$, and the fluctuating portion u'. From the three parts, statistical quantities such as the ensemble-averaged velocity $\langle U \rangle$ and the standard deviation from the ensemble average $u'_{\text{sd}} = (\langle u'(x, \phi)^2 \rangle)^{1/2}$ as a function of phase angle ϕ were determined.[13] About 100 oscillation cycles of data were measured for each ensemble-averaged quantity.

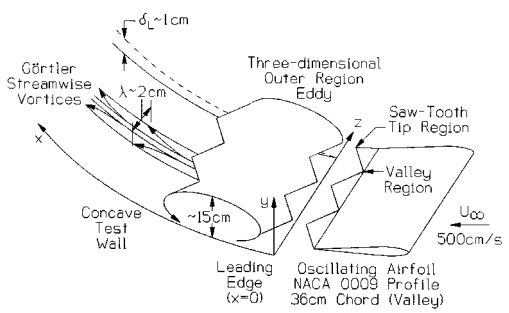

Fig. 1 Emulation method and experimental situation.

Results and Discussion

When an airfoil with a sawtooth trailing edge is pitch oscillated, the resulting shed vortex is three dimensional and complicated. Myose and Iwata[14] conducted a dye flow-visualization experiment in a water tunnel under dynamically similar conditions, i.e., the same reduced oscillation frequency. At the start of pitchdown motion, i.e., $\phi = 0$, a seepage of fluid moving from the upper to the lower surface at the valley region was found. This downward fluid motion (akin to an insweep) first occurs in the valley region before spreading to the tip region. This seepage motion becomes a circulatory motion, which results in a bound vortex generally aligned with the sawtooth trailing edge. When the pitch direction is changed, the vortex over the valley region is shed immediately, whereas the vortex over the tip region remains over the airfoil for a short time. This results in a three-dimensional outer eddy skewed in the spanwise direction as illustrated in Fig. 1.

The interaction between near-wall vortices and outer-region eddy is shown by the flow-visualization result of Fig. 2. The smoke-wire technique results in a series of highly visible white smoke lines consisting of vaporized oil particles carried along by the flow. The individual smoke lines remain distinct and parallel to the flow when there is no mixing or spanwise flow. Although Görtler vortices produce streamwise swirling motion, these vortices are relatively weak so that their effect is not easily visible by the downstream location shown in Fig. 2.

For $\phi \gtrsim 1.75\pi$, flow visualization showed some fluctuations in the smoke in the valley region. Figure 2 shows that violent mixing of the smoke ensued for $\phi \gtrsim 0$. During the same time period, Fig. 2 shows that the tip region is generally undisturbed. According to water-tunnel observations, wallward fluid motion occurs in the valley region at the start of pitchdown ($\phi \gtrsim 0$) but not in the tip region. Thus, this violent mixing of smoke in the valley region is due to the arrival of high-speed fluid associated with the large outer eddy. During phase angles of $0 \lesssim \phi \lesssim 0.5\pi$, flow-visualization results indicate the presence of spanwise w velocity, which moves smoke lines away from the valley and toward the tips. This is consistent with the spread of circulatory motion from the valley to the tips observed in the water-tunnel experiment. In the later part of the large outer eddy, the valley region becomes devoid of smoke as the high-speed sweep clears away the smoke. Shortly thereafter in time, undisturbed wall vortices return, and the entire process is repeated during the next phase cycle.

Figure 3 shows isocontours of $\langle U \rangle / U_\infty$ and u'_{sd}/U_∞ at $x = 82.5$ cm, $y = 0.3$ cm ($y^+ = 34$) for the sawtooth valley centered at $z = 9.5$ cm. During the later part of the phase cycle ($\phi \gtrsim 1.3\pi$), Fig. 3a shows low-speed streaks centered at $z \approx 8.8$ and 9.8 cm. For $\phi \gtrsim 1.7\pi$ in Fig. 3b, there are moderately high standard deviations ($u'_{\text{sd}}/U_\infty > 0.05$) to the spanwise sides of the low-speed streak ($z \approx 9.5$ and 10 cm). This is consistent with the appearance of fluctuating smoke lines centered around the valley in the flow-visualization results. Violent mixing of the smoke followed these prebreakdown fluctuations. An indicator of breakdown is cessation of the streak structure during $0.2\pi \lesssim \phi \lesssim 1.2\pi$ in Fig. 3a. This was accompanied by the presence of high standard deviation ($u'_{\text{sd}}/U_\infty > 0.1$), which occurs during $0 \lesssim \phi \lesssim \pi$ in Fig. 3b. Note that the highest standard deviation ($u'_{\text{sd}}/U_\infty \approx 0.2$) occurs at $\phi \approx 0.2\pi$

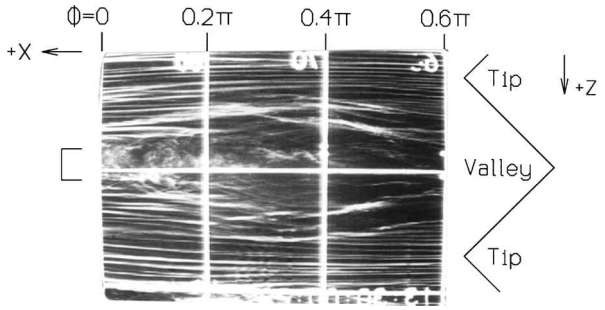

Fig. 2 Flow visualization of the interaction: Photograph is mirror imaged; horizontal and vertical grid lines shown are 10 cm apart; sawtooth valley located at z = 9.5 cm (near the middle horizontal line). The spanwise extent of the data in Fig. 3 is indicated by [.

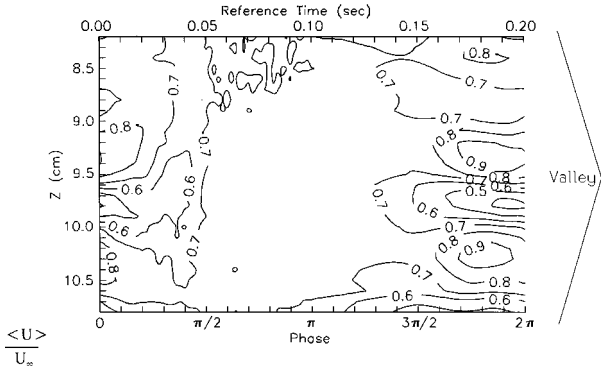

a) Isocontours of the ensemble-averaged velocity

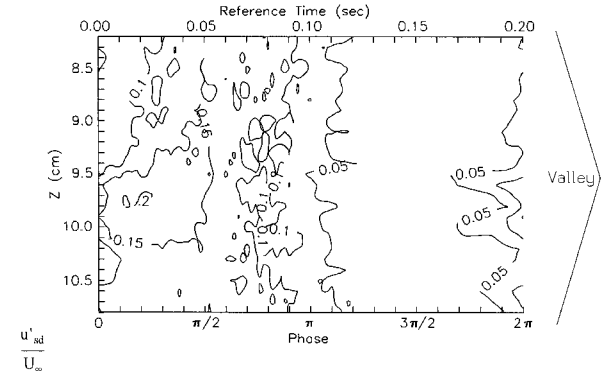

b) Standard deviation

Fig. 3 Quantitative results of the interaction taken at $x = 82.5$ cm, $y = 0.3$ cm ($y^+ = 34$): Saw-tooth valley is located at $z = 9.5$ cm.

centered about the low-speed streak ($z \approx 9.8$ cm). Because the high-speed wallward (insweep) motion occurs at $\phi \approx 0$, the wall eddy breaks down soon after the arrival of the insweep at that location.

Breakdown phase angles were quite different for wall eddies located near the sawtooth tip. In this case, the streak structure was terminated during $0.4\pi \lesssim \phi \lesssim \pi$, which is shorter in duration than the valley region. This difference in breakdown phase angle was due to the late arrival of the high-speed insweep at the tip location. Thus, breakdown of wall eddy is driven by the arrival of the high-speed insweep, which is associated with the three-dimensional, outer-region structure.

Summary

An experiment to study the interactive effect of large, three-dimensional outer eddies on small streamwise vortices was conducted. The TBL near-wall structure was emulated by Görtler streamwise vortices. Outer-region, three-dimensional eddies were shed from the pitch oscillation of an airfoil with sawtooth trailing edge. The three-dimensional eddies included skewed leading and trailing edges and a wallward motion similar to insweeps observed in TBLs. The interaction involved fluctuation of the near-wall structure as the outer eddy approached. Violent mixing of fluid and breakdown of the near-wall structure ensued as high-speed fluid associated with the outer eddy arrived. This suggests that the insweep associated with the outer region helps trigger the bursting of the near-wall structure in bounded turbulent shear flows.

Acknowledgments

This work was sponsored by the Office of Naval Research under Contract N00014-89-J-1400 and the U.S. Air Force Office of Scientific Research under Contract F49620-85-C-0080.

References

[1]Cantwell, B. J., "Organized Motion in Turbulent Flow," *Annual Review of Fluid Mechanics*, Vol. 13, 1981, pp. 457–515.

[2]Robinson, S. K., "Coherent Motions in the Turbulent Boundary Layer," *Annual Review of Fluid Mechanics*, Vol. 23, 1991, pp. 601–639.

[3]Kline, S. J., Reynolds, W. C., Schraub, F. A., and Runstadler, P. W., "The Structure of Turbulent Boundary Layers," *Journal of Fluid Mechanics*, Vol. 30, Dec. 1967, pp. 741–773.

[4]Bogard, D. G., and Tiederman, W. G., "Characteristics of Ejections in Turbulent Channel Flow," *Journal of Fluid Mechanics*, Vol. 179, June 1987, pp. 1–19.

[5]Acarlar, M. S., and Smith, C. R., "A Study of Hairpin Vortices in a Laminar Boundary Layer. Part 1. Hairpin Vortices Generated by a Hemisphere Protuberance," *Journal of Fluid Mechanics*, Vol. 175, Feb. 1987, pp. 1–41.

[6]Swearingen, J. D., and Blackwelder, R. F., "The Growth and Breakdown of Streamwise Vortices in the Presence of a Wall," *Journal of Fluid Mechanics*, Vol. 182, Sept. 1987, pp. 255–290.

[7]Blackwelder, R. F., and Kovasznay, L. S., "Time Scales and Correlations in a Turbulent Boundary Layer," *Physics of Fluids*, Vol. 15, Sept. 1972, pp. 1545–1554.

[8]Brown, G. L., and Thomas, A. S. W., "Large Structure in a Turbulent Boundary Layer," *Physics of Fluids*, Vol. 20, Oct. 1977, pp. S243–S252.

[9]Chen, C. P., and Blackwelder, R. F., "Large-Scale Motion in a Turbulent Boundary Layer: A Study Using Temperature Contamination," *Journal of Fluid Mechanics*, Vol. 89, Nov. 1978, pp. 1–31.

[10]Praturi, A. K., and Brodkey, R. S., "A Stereoscopic Visual Study of Coherent Structures in Turbulent Shear Flow," *Journal of Fluid Mechanics*, Vol. 89, Nov. 1978, pp. 251–272.

[11]Smith, C. R., "Visualization of Turbulent Boundary-Layer Structure Using a Moving Hydrogen Bubble-Wire Probe," *Coherent Structures of Turbulent Boundary Layers*, edited by C. R. Smith and D. E. Abbott, Lehigh Univ. Press, Bethlehem, PA, 1978, pp. 48–97.

[12]Falco, R., "The Production of Turbulence Near a Wall," AIAA Paper 80-1356, July 1980.

[13]Myose, R. Y., and Blackwelder, R. F., "On the Role of the Outer Region in the Turbulent-Boundary-Layer Bursting Process," *Journal of Fluid Mechanics*, Vol. 259, Jan. 1994, pp. 345–373.

[14]Myose, R. Y., and Iwata, J., "Flow Visualization of an Oscillating Airfoil with Saw-Tooth Trailing Edge," *AIAA Journal*, Vol. 34, No. 9, 1996, pp. 1748–1750.

F. W. Chambers
Associate Editor

Constrained Damage Detection Technique for Simultaneously Updating Mass and Stiffness Matrices

Jason Kiddy* and Darryll Pines†
University of Maryland,
College Park, Maryland 20742-3015

Introduction

OVER the past 10 years, a considerable amount of attention has been paid to modal-based damage detection algorithms. In most instances, the damage detection problem is simplified to the detection and characterization of stiffness failures. However, several authors have attempted to simultaneously classify both mass and stiffness changes.[1,2] Recently, it has been noted that modal data cannot be used to correctly identify these combined failures due to the nonunique nature of the mode shapes.[3] This arbitrary scaling of the mode shapes creates an infinite number of mass and stiffness matrices that satisfy the eigenvalue equation. However, it will be shown that it is possible to perform simultaneous updating of both matrices if the problem is properly constrained.

Received Dec. 11, 1997; revision received March 14, 1998; accepted for publication March 28, 1998.

*Graduate Fellow, Department of Aerospace Engineering. Student Member AIAA.

†Assistant Professor, Department of Aerospace Engineering. Senior Member AIAA.